Heliyon 9 (2023) e17810

Contents lists available at ScienceDirect

Heliyon

journal homepage: www.cell.com/heliyon

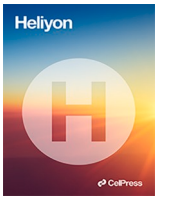

Binary glycerol-based deep eutectic solvents containing zinc nitrate hexahydrate salt for rechargeable zinc air batteries applications with enhanced properties

Fentahun Adamu Getie [a,b], Delele Worku Ayele [a,c,*], Nigus Gabbiye Habtu [a,d,**], Fantahun Aklog Yihun [e], Temesgen Atnafu Yemata [d], Mehary Dagnaw Ambaw [e], Ababay Ketema Worku [a]

[a] Bahir Dar Energy Center, Bahir Dar Institute of Technology, Bahir Dar University, P.O. Box 26, Bahir Dar, Ethiopia
[b] Department of Chemistry, College of Natural and Computational Science, Injibara University, P.O. Box 40, Injibara, Ethiopia
[c] Department of Chemistry, College of Science, Bahir Dar University, P.O. Box 79, Bahir Dar, Ethiopia
[d] Faculty of Chemical Engineering, Bahir Dar Institute of Technology, Bahir Dar University, P.O. Box 26, Bahir Dar, Ethiopia
[e] Department of Industrial Chemistry, College of Science, Bahir Dar University, P.O. Box 79, Bahir Dar, Ethiopia

ARTICLE INFO

Keywords:
Zinc nitrate hexahydrate salt
Glycerol
Deep eutectic solvent
Heating method
Rechargeable zinc air batteries

ABSTRACT

Deep eutectic solvents (DESs) have attracted interest due to their unique and favorable electrochemical characteristics. This study reported a novel binary glycerol-zinc salt deep eutectic solvents were prepared with a combination of hydrogen bond donor (glycerol (Gly)) and hydrogen bond acceptor (Zinc nitrate hexahydrate (ZNH)) at different molar ratios of 1:2, 1:3, 1:4, 1:5, and 1:6. The various physicochemical properties including viscosity, refractivity index, conductivity, thermogravimetric analysis (TGA), Fourier transform infrared spectroscopy (FTIR), cyclic voltammetry (CV) and electrochemical impedance (EIS) were measured. The results showed that among the various combinations tested, DES 1:2 resulted in a low viscosity value of 690, 500, 310, 220, and 160 mPa (mPa s) at shear rate (s^{-1}) values of 20, 30, 60, 100, and 200 respectively. Moreover, DES 1:2 resulted in more electrochemically stable solvents with a lower refractive index value of 1.446, and a higher conductivity (σ) of 4.41 mS/cm. The findings found disclose the features, nature and of properties of prepared DESs as a potential solvents for different electrochemical storage applications.

1. Introduction

The rapidly increasing environmental pollution and energy crisis have resulted in an urgent need for alternative green and renewable energy resources including tidal, solar, and wind energy [1]. So far, there has been a demand for an efficient, dependable, and safe energy storage method to improve energy conversion in power plants [2]. To date, batteries have fascinated great attention because of their low cost, safety, charge storage efficiency, outstanding cyclic durability, design diversity, and clean electrical energy storage systems [3,4]. Moreover, a rise in the degree of electrification in different uses such as electric vehicles, portable electronic

* Corresponding author. Bahir Dar Energy Center, Bahir Dar Institute of Technology, Bahir Dar University, P.O. Box 26, Bahir Dar, Ethiopia.
** Corresponding author. Bahir Dar Energy Center, Bahir Dar Institute of Technology, Bahir Dar University, P.O. Box 26, Bahir Dar, Ethiopia.
E-mail addresses: delelewww@gmail.com (D.W. Ayele), nigusgabiye@bdu.edu.et (N.G. Habtu).

https://doi.org/10.1016/j.heliyon.2023.e17810
Received 11 February 2023; Received in revised form 27 June 2023; Accepted 28 June 2023
Available online 30 June 2023

devices and electric appliances attracted the use of batteries [5]. Several batteries, like the lithium-ion battery, nickel-metal hydride battery, and the lead-acid batteries have already been commercialized. However, these batteries are still expensive. Moreover, there are issues concerning safety, raw material source, and toxicity [6]. Among the electrode materials, zinc is relatively inexpensive, abundant, and environmentally friendly. A zinc air battery (ZAB) is of interest among metal-air batteries due to its environmental friendliness, high energy density, high safety, and low cost [7,8]. Electrolytes are essential functional components for rechargeable zinc air batteries to establish ionic and electronic circuits between the cathode and anode [1]. In general, alkaline electrolytes have been widely used in rechargeable zinc air batteries (RZABs) due to their higher energy densities, low viscosity, high ionic conductivity and desirable kinetics for both the oxygen reduction reaction (ORR) and oxygen evolution reaction (OER) and they provide excellent electrochemical properties [9,10]. However, the main issues in alkaline electrolytes are dissolution of Zn, hydrogen evolution, dendrite growth, passivation, shape changes, and precipitation of insoluble carbonates [2]. Therefore, the development of low-cost, safe, and high-performance electrolyte materials is urgently needed to keep up with the rapid growth of electrochemical energy storage applications [11].

Currently, deep eutectic solvents (DESs) are non-alkaline solvents prepared by simple mixing, eliminating the need for complicated synthesis through hydrogen bond interactions [12]. Recent research has shown DESs can be used as electrolytes due to many characteristics such as low vapor pressure [13], facile preparation [11], low cost [14], good solubility [1], good thermal and chemical stability [15], non-flammability, better environmental compatibility, a wider electrochemical window than aqueous electrolytes, and providing a higher energy density [16].

Many studies have been published on DESs for various energy storage applications, like the fabrication of nanomaterial's for energy storage technologies [17], conversion technology/electrochemical energy storage in electrolytes [18], batteries [19], supercapacitors applications [20], hierarchical carbon electrodes for fuel cells [21], solar energy technologies [22] and functional material synthesis for energy storage purposes [23]. Hence, all the above-mentioned issues enable DESs to be a promising functional electrolyte for electrochemical energy conversion and storage. However, no reports have been available on type IV DESs; particularly ZNH/Gly based DESs as an electrolyte for battery energy storage systems. Because of its low cost, freezing point suppressants, viscosity modifiers, biodegradability, nontoxicity, and non-flammability, the use of glycerol as a prospective HBD in the development of DESs has attracted a lot of attention [24]. In this study, we developed a low-cost binary ZNH/Gly)-based DES as an electrolyte for RZABs.

2. Experiment

2.1. Chemicals

Zinc nitrate hexahydrate (ZNH) (96%, LOBA-Chemie) and glycerol (Gly) (neo-lab life science, 99.0%) were used for the synthesis of DESs. These chemicals were employed without further purification. All the chemicals used were analytical grade reagents.

2.2. DESs synthesis

ZNH based DESs were synthesized by mixing ZNH ($Zn(NO_3)_2.6H_2O$) salt with Gly($C_3H_8O_3$) at a various molar ratio of 1:2,1:3, 1:4,1:5 &1:6, respectively. They were prepared using a facile heating preparation method (Fig. 1). The ratio of ZNH salts to Gly was determined based on the stability and homogeneity of the DES. The mixtures of ZNH salts to Gly were maintained at 90 °C for 1 h and resulted in a clear homogenous liquid. Then, the obtained DESs were left to cool to room temperature, kept in closed laboratory vials, and stored inside a desiccator for further analysis.

2.3. Characterization

The conductivity measurements were performed using a conductivity meter (Vlirous model VWR-PH enominal Mu6100H) at 298.15 K. It was calibrated with conductivity standard of 1413 μS/cm. The viscosities of all DESs were measured by using viscometer (Brookfield LV DV-II + Pro, USA). The refractive index measurements of the investigated DESs were measured using Abe refractometer (model AT1167) utilizing sodium light beam at 298.15. The Fourier Transform Infrared spectroscopy (FTIR) (JASCO MODEL FT/IR-6600 type A) was employed at 4 cm^{-1} resolution and wavelength range of 400–4000 cm^{-1} to analyze the functional groups in ZNH/

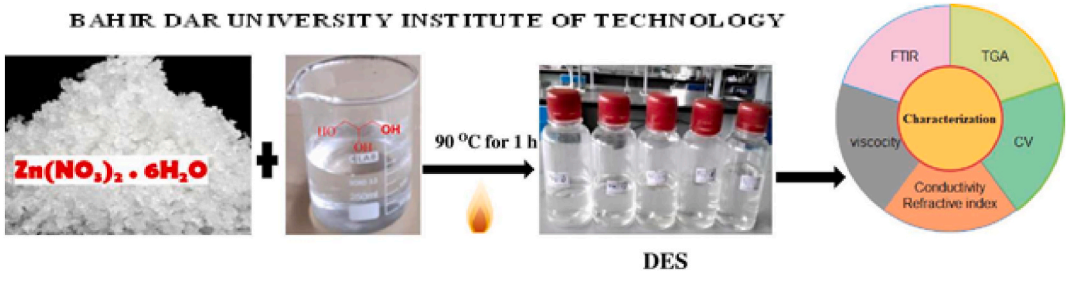

Fig. 1. Schematic illisturation for the synthesis ZNH/GLY based DESs by heating method.

Gly based DESs. To check the thermal stability, thermogravimetric analysis (TGA) of DESs was performed using BJHENVEN HCT-1 to analyze the thermal stability. It was measured in nitrogen atmosphere in a temperature range of 25–600 °C. Cyclic voltammetry (CV) measurements were done using an (METEROHM MULTI AUTOLAB M204, MAC90083, and Netherlands) with NOVA software in a 3-electrode electrochemical cell. It comprises quasi Ag/AgCl reference electrode, Pt wire counter electrode and glassy carbon working electrode (3 mm diameter). The working electrode was carefully polished with alumina suspensions (0.25 mM) and rinsed in distilled water before each voltammetry measurement. All cyclic voltammograms were recorded at a scan rate of 10 and 20 mV/s. The frequency range of the electrochemical impedance spectroscopy measurement varies from 0.01 Hz to 100 Hz.

3. Result and discussion

3.1. Physicochemical properties

3.1.1. Conductivity measurements

The conductivity (σ) of DESs is a vital transport characteristic in electrochemical applications. The σ is affected by viscosity, concentration of charge carriers, and ion mobility [25]. The σ of the ZNH/GLY based DESs at different molar ratios covers a σ range from 1.39 to 4.41 mS/cm (Table 1). The σ increased with the decrease in their viscosities since the σ pattern of DESs is influenced by their ion mobility [26]. The mixtures of Gly and ZNH form room temperature molten liquids in a certain composition range. The composition has been optimized using the σ of the mixtures that are liquids at 298 K and the stability of the molten electrolyte as a liquid without any spontaneous crystallization under ambient conditions. Fig. 2 shows the variation of σ as a function of ZNH/Gly concentration [24]. The increasement of the mole fraction of ZNH up to 0.33 in the ternary mixture resulted in an increased σ. It is found that 0.33 mol fraction of ZNH and 0.66 mol fraction of Gly yield the best possible σ with lower viscosity. This could be due to creation of a larger free volume (i.e., weaker intermolecular hydrogen bond) between the HBA and HBD at the optimal concentrations. While beyond 0.33 mol fraction of ZNH resulted in decrease σ and that could be due to the formation of crystals in the ternary mixture. The highest σ values of 4.41 mS/cm obtained at 298 K at the optimized composition 0.33 mol fraction of ZNH and 0.66 mol fraction of Gly (DES1:2) of among the DESs. This value was in good agreement with the reported literature somewhere else [27]. The σ values of the DESs followed the order of DES1:2 > DES1:3 > DES1:4 > DES 1:5 > DES1:6 (Table 1).

3.1.2. Viscosity

Viscosity is the crucial transport characteristics of DESs that defines the internal resistance of a fluid to shear stress [28]. The hydrogen bonding strength, the nature of HBD, and the salt/HBD mole ratio determine the viscosity of DESs [29]. The viscosity values decreased in the order of DES 1:6 > DES 1:5 > DES 1:4 > DES 1:3 > DES 1:2 (Fig. 2 and Table 1). The results show that the viscosity of DES increased as the molar ratio of glycerol increased. This could be due to the more hydrogen bond interactions, the increase in the attractive force and the decrease in the free volume of DES because of the presence of more glycerol [30]. The lowest viscosity value was obtained for DES1:2 (Fig. 2 and Table 1). This can be due to the formation of weak intermolecular hydrogen bonds between ZNH and Gly [31]. The low viscosity value is favorable for DESs electrolytes in electrochemical systems as it provides the free mobility of ionic species [32]. While DES1:6 resulted in a higher viscosity value compared to DES1:5, DES1:4, DES1:3, and DES 1:2. This could be attributed to the higher polarity of ZNH and Gly which results in less mobility as well as an increase in the number of contributing substances in the formation of hydrogen bonds [27]. Furthermore, shear rate ($\mathbf{s^{-1}}$) influences the viscosity of the DES (Fig. 3). It shows that as shear rate increased the viscosity values decreased that indicates shear thinning behavior and this agrees with previous reported research [33].

3.1.3. Refractive index measurements

It is a vital characteristics of the solvent which defines the index, optical property, and purity concentration of solute in solvent [34]. The refractive index (RI) values of the synthesized ZNH/Gly ranges in 1.446–1.470 (Table 1) and the result is similar to previous works reported somewhere else [21]. Table 1 demonstrates that the RI increased as the molecular ratio of the DES increased. This could be the higher molar ratios that resulted in a reduced vacant holes or spaces between particles in ZNH or Gly solutions that restrict particle movement [27].

Table 1
Composition and physicochemical properties DESs at various molar ratios.

Composition	Abbrev-iation	σ (mS/cm) at 25 °C	Viscosity (mPa s) at 25 °C					Refractive index (20 °C)	Physical state (solution)
			Shear rate ($_S{}^{-1}$)						
			20	30	60	100	200		
ZNH/Gly (1:2)	DES1:2	4.41 ± 0.01	690	500	310	220	160	1.446 ± 0.002	Clear
ZNH/Gly (1:3)	DES1:3	3.32 ± 0.02	720	520	340	270	210	1.459 ± 0.0015	Clear
ZNH/Gly (1:4)	DES1:4	1.76 ± 0.03	880	710	490	410	350	1.464 ± 0.001	Clear
ZNH/Gly(1:5)	DES1:5	1.42 ± 0.01	910	790	540	470	410	1.466 ± 0.0025	Clear
ZNH/Gly(1:6)	DES1:6	1.39 ± 0.015	920	810	570	490	450	1.470 ± 0.003	Clear

Note: ZNH: Zinc nitrate hexahydrate, Gly: glycerol, mPa s: milliPascal, DES: deep eutectic solvent.

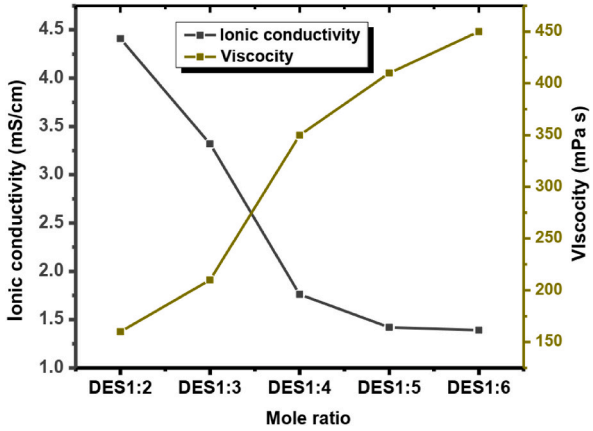

Fig. 2. Correlation between σ and viscosity vs. ZNH/Gly molar ratio in DESs.

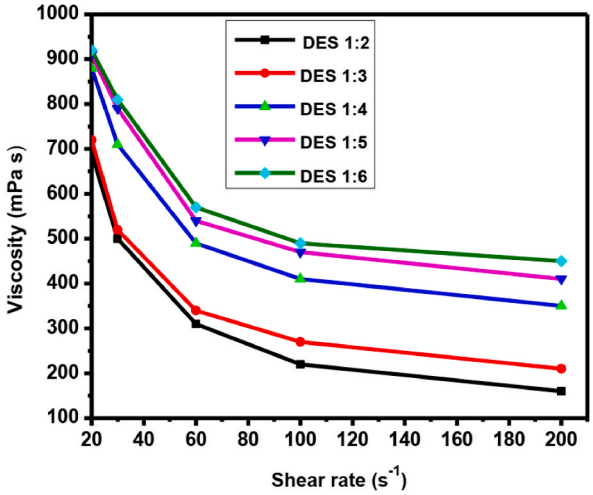

Fig. 3. Change in viscosity as a function of shear rate.

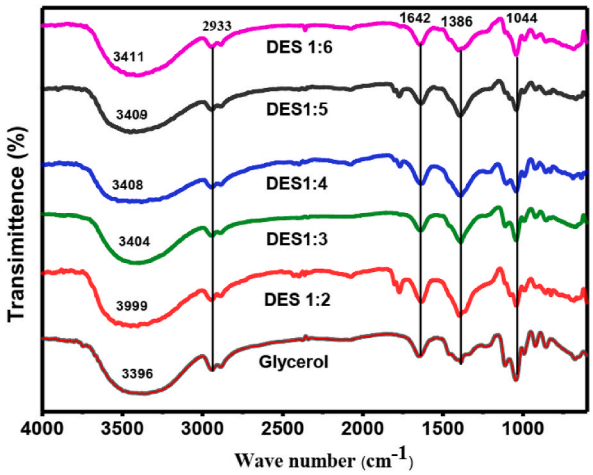

Fig. 4. FTIR spectra for ZNH/Gly based DESs and pure glycerol.

3.1.4. FTIR analysis

Fig. 4 shows FTIR spectra obtained for mixtures of ZNH and Gly in various compositions. The analysis of the absorbance values, band widths, and frequency shifts of the same bond in various combinations can help in the interpretation of DES structures. The broad peak around at 3396 - 3411 cm^{-1} were attributed to the hydrogen bond formation of DES, which could be obtained from the absorbed hydroxyl group of $C_3H_8O_3$ and $Zn(NO_3)_2.6H_2O$. The ethyl group v(C–H) stretching vibration occurred at 2933 cm^{-1} while the v(C–H) bending absorption of CH_2 peaks was observed at 1386 cm^{-1}. The peak at 1044 cm^{-1} is assigned the v(C–O) stretching bandwidth alcohol group in GLY. The strong peak at 1642 cm^{-1} is due to the v(H–*O*–H), which is formed by a water molecule in $Zn(NO_3)_2.6H_2O$ [27].

3.1.5. Thermal stability analysis

The thermal stability of as-prepared DESs in terms of decomposition temperature was obtained using TGA analysis [35]. The TGA of ZNH/Gly showed three main steps during its thermal decomposition, as illustrated in Fig. 5. The first weight loss prior to 180 °C was attributed to the vaporation of the hydrated water content of ZNH/Gly-based DESs. The second mass loss in the temperature ranges of 183–316 °C was obtained, and it can be due to the evaporation of glycerol [36]. The Zn eutectic solvent loses its organic component instead of decomposing as the temperatures close to the boiling point of pure organic constituents [37]. The third mass loss in (320–433 °C) is observed due to the decomposition of as-prepared ZNH/Gly during the heating stage. After 433 °C, there is no weight loss in the DES, indicating that the ZNH/Gly DES might be transformed to ZnO. DES 1:2 showed the lowest thermal stability of the ZNH/Gly DES system, while DES 1:6 was found to be highly stable. The thermal stability decreased in the order of: DES 1:4 < DES 1:2 < DES 1:3 < DES 1:5 < DES 1:6 < pure Gly (Fig. 5). This pattern might be related to the increasing number of intermolecular interaction of hydrogen bonds formed between ZNH and Gly [27,38], showing the molar ratios of DESs and intermolecular interaction between ions have a significant impact on thermal stability.

3.2. Electrochemical study

3.2.1. Cyclic voltammetry of DESs

As shown in Fig. 6 (a - e), cyclic voltammetry for ZNH/Gly based DESs at various molar ratios revealed the reversibility of DESs towards oxidation and reduction reactions within the potential range of −1.0 to +1.2 V, allowing the selection of the appropriate electrolyte for rechargeable zinc air batteries [39]. The reversibility of the reactions of ZNH/Gly-based DESs were investigated using a three-electrode configuration system consisting of glassy C (working electrode), Pt wire (counter electrode), and quasi-Ag/AgCl (reference electrode) immersed in ZHN/Gly electrolytes. The CV study for DES 1:2 at 10 and 20 mV validated the electrochemical stability towards reduction and oxidation reactions within the potential range of −1.0 to +1.2 V, as shown in Fig. 6a [40]. A subsequent oxidation peaks were observed for DES1:3, DES1:4, DES1:5 and DES1:6 respectively are not electrochemically stable compared to DES 1:2 [41–43].

3.2.2. Impedance spectroscopy analysis (EIS)

Fig. 7, also shows the Nyquist plot (Z′ vs. Z″), which is a frequency response plot used to evaluate the ionic conductivity of a ZNH/Gly system at room temperature. Nyquist plots are divided into three regions: the semicircle at high frequencies, which is the interfacial charge transfer region, diffusion, and the capacitive region. The semicircles of the Nyquist plots for the ZNH/Gly deep eutectic solvents were unnoticeable. This was due to the low charge transfer resistance at the electrode-electrolyte interfaces [44]. Finally, the conductivities of ZNH/DESs at room temperature measured with a conductivity meter (Vlirous model VWR-PH enominal 4 Mu6100H)

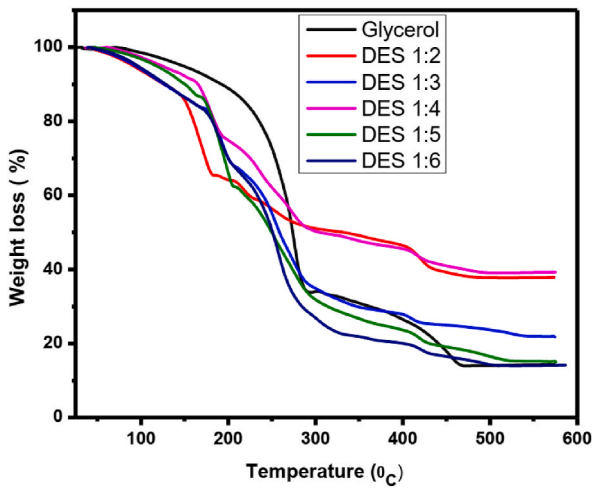

Fig. 5. Thermal degradation curves for ZNH/Gly DES and pure glycerol.

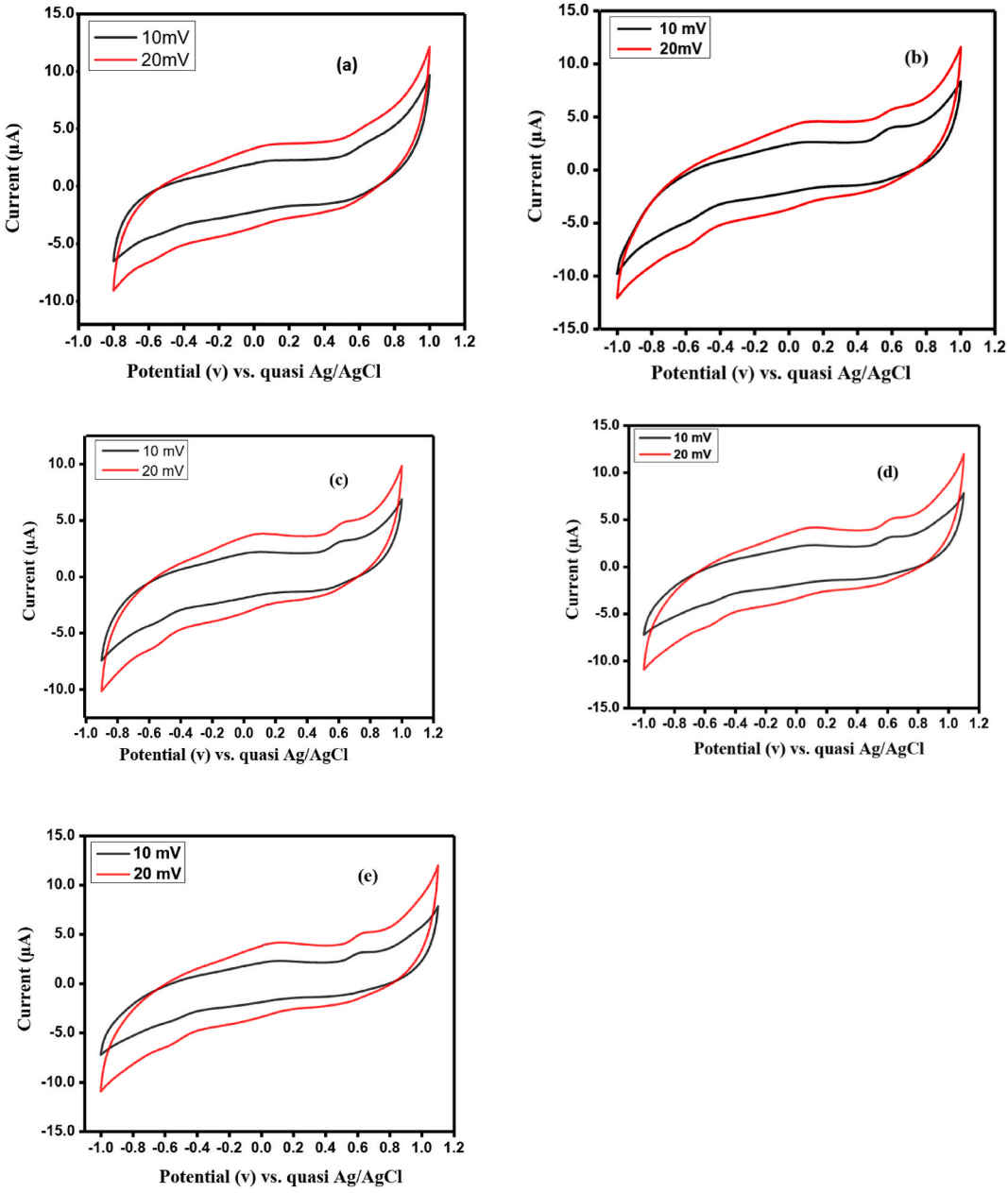

Fig. 6. CV curves of; **(a)** DES1:2 **(b)** DES1:3 **(c)** DES1:4 **(d)** DES1:5 **(e)** DES1:6 at 10 mV/s and 20 mV/s.

are.4.41, 3.32, 1.76, 1.42, and 1.39 mS/cm for DES1:2, DES1:3, DES1:4, DES1:5, and DES1:6, respectively (Table 1).

4. Conclusions

In this study, electrochemically reversible ZNH/GLY-based DESs were synthesized with GLY as the HBD and zinc salt as the HBA. The results showed that the nature and molar ratios of the GLY and ZNH salts influenced the eutectic properties of ZNH/GLY based DESs, which played a vital role in the physicochemical property of the resulting ternary DESs. DES1:2 was the best electrolyte in terms of viscosity, refractive index, and maximum conductivity (4.41 mS/cm). The anodic and cathodic peaks of DES1:2 were not clearly observed in the potential range of −1.0 to 1.2 V and it exhibited a wider and more electrochemically stable electrolyte than other samples. Furthermore, the semicircles of the Nyquist plots for the ZNH/Gly DESs were barely visible. This was due to the electrode-electrolyte interface's resulting in an extremely low charge transfer resistance. Finally, the σ of ZNH/DESs was measured at room temperature using a conductivity meter. Hence, the high σ, low viscosities, and the electrochemical stability towards oxidation and

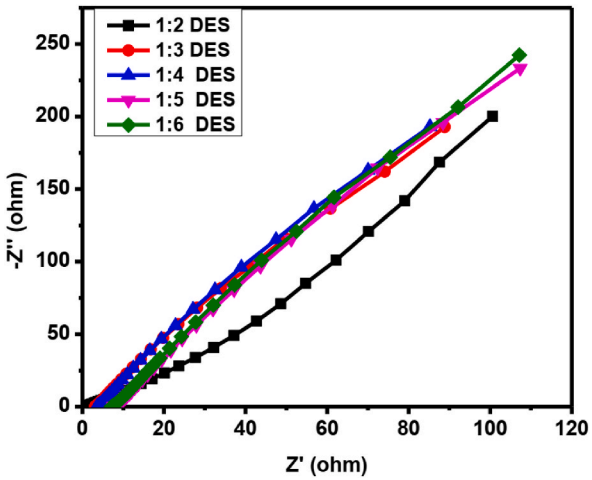

Fig. 7. Nyquist plot of ZNH/GLY based different molar ratios of DESs.

reduction reaction for DES 1:2 make them a promising candidate for different industrial application.

Author contribution statement

Fentahun Adamu Getie: Conceived and designed the experiments; Performed the experiments; Analyzed and interpreted the data; Wrote the paper,.Delele Worku Ayele, Nigus Gabbiye Habtu: Analyzed and interpreted the data; Contributed reagents, materials, analysis tools or data; Wrote the paper,.Fantahun Aklog Yihun, Temesgen Atnafu Yemata, Ababay Ketema Worku: Analyzed and interpreted the data; Wrote the paper,.Mehary Dagnew Ambaw: Conceived and designed the experiments; Wrote the paper.

Additional information

No additional information is available for this paper.

Declaration of competing interest

The authors declare that they have no known competing financial interests or personal relationships that could have appeared to influence the work reported in this paper.

Acknowledgements

The authors acknowledge Bahir Dar Institute Technology and Injibara University for financial and chemical support.

References

[1] J. Wu, Q. Liang, X. Yu, Q. Lü, L. Ma, X. Qin, G. Chen, B. Li, Deep eutectic solvents for boosting electrochemical energy storage and conversion : a review and perspective, Adv. Funct. Mater. (2021), 2011102, https://doi.org/10.1002/adfm.202011102, 1–25.
[2] F. Adamu, G. Delele, W. Ayele, N.G. Habtu, F.A. Yihun, Development of electrolytes for rechargeable zinc - air batteries : current progress , challenges , and future outlooks, SN Appl. Sci. (2022), https://doi.org/10.1007/s42452-022-05156-z.
[3] X.F. Lu, Y. Fang, D. Luan, X.W.D. Lou, Metal–organic frameworks derived functional materials for electrochemical energy storage and conversion: a mini review, Nano Lett. 21 (2021) 1555–1565, https://doi.org/10.1021/acs.nanolett.0c04898.
[4] K.T.T. Tran, L.T.M. Le, A.L.B. Phan, P.H. Tran, T.D. Vo, T.T.T. Truong, N.T.B. Nguyen, A. Garg, P.M.L. Le, M.V. Tran, New deep eutectic solvents based on ethylene glycol - LiTFSI and their application as an electrolyte in electrochemical double layer capacitor (EDLC), J. Mol. Liq. 320 (2020), 114495, https://doi.org/10.1016/j.molliq.2020.114495.
[5] G. Zubi, R. Dufo-López, M. Carvalho, G. Pasaoglu, The lithium-ion battery: state of the art and future perspectives, Renew. Sustain. Energy Rev. 89 (2018) 292–308, https://doi.org/10.1016/j.rser.2018.03.002.
[6] D. Larcher, J.M. Tarascon, Towards greener and more sustainable batteries for electrical energy storage, Nat. Chem. 7 (2015) 19–29, https://doi.org/10.1038/nchem.2085.
[7] C. Zhong, B. Liu, J. Ding, X. Liu, Y. Zhong, Y. Li, C. Sun, X. Han, Y. Deng, N. Zhao, W. Hu, Decoupling electrolytes towards stable and high-energy rechargeable aqueous zinc–manganese dioxide batteries, Nat. Energy 5 (2020) 440–449, https://doi.org/10.1038/s41560-020-0584-y.
[8] J. Pan, Y.Y. Xu, H. Yang, Z. Dong, H. Liu, B.Y. Xia, Advanced architectures and relatives of air electrodes in Zn–air batteries, Adv. Sci. 5 (2018), https://doi.org/10.1002/advs.201700691.
[9] X. Liu, X. Fan, B. Liu, J. Ding, Y. Deng, X. Han, C. Zhong, W. Hu, Mapping the design of electrolyte materials for electrically rechargeable zinc–air batteries, Adv. Mater. 33 (2021) 1–21, https://doi.org/10.1002/adma.202006461.
[10] A.K. Worku, D.W. Ayele, N.G. Habtu, M.D. Ambaw, Engineering nanostructured Ag doped α-MnO2 electrocatalyst for highly efficient rechargeable zinc-air batteries, Heliyon 8 (2022), https://doi.org/10.1016/j.heliyon.2022.e10960.

[11] C. Zhang, L. Zhang, G. Yu, Eutectic electrolytes as a promising platform for next-generation electrochemical energy storage, Acc. Chem. Res. 53 (2020) 1648–1659, https://doi.org/10.1021/acs.accounts.0c00360.
[12] H. Ogawa, H. Mori, Lithium salt/amide-based deep eutectic electrolytes for lithium-ion batteries: electrochemical, thermal and computational study, Phys. Chem. Chem. Phys. 22 (2020) 8853–8863, https://doi.org/10.1039/d0cp01255f.
[13] B.B. Hansen, S. Spittle, B. Chen, D. Poe, Y. Zhang, J.M. Klein, A. Horton, L. Adhikari, T. Zelovich, B.W. Doherty, B. Gurkan, E.J. Maginn, A. Ragauskas, M. Dadmun, T.A. Zawodzinski, G.A. Baker, M.E. Tuckerman, R.F. Savinell, J.R. Sangoro, Deep eutectic solvents: a review of fundamentals and applications, Chem. Rev. 121 (2021) 1232–1285, https://doi.org/10.1021/acs.chemrev.0c00385.
[14] L. Zhang, C. Zhang, Y. Ding, K. Ramirez-Meyers, G. Yu, A low-cost and high-energy hybrid iron-aluminum liquid battery achieved by deep eutectic solvents, Joule 1 (2017) 623–633, https://doi.org/10.1016/j.joule.2017.08.013.
[15] H. Ghaedi, M. Ayoub, S. Sufian, B. Lal, Y. Uemura, Thermal stability and FT-IR analysis of Phosphonium-based deep eutectic solvents with different hydrogen bond donors, J. Mol. Liq. 242 (2017) 395–403, https://doi.org/10.1016/j.molliq.2017.07.016.
[16] X. Ge, C. Gu, X. Wang, J. Tu, Deep eutectic solvents (DESs)-derived advanced functional materials for energy and environmental applications: challenges, opportunities, and future vision, J. Mater. Chem. A. 5 (2017) 8209–8229, https://doi.org/10.1039/c7ta01659j.
[17] A. Ray, B. Saruhan, Application of ionic liquids for batteries and supercapacitors, Materials 14 (2021), https://doi.org/10.3390/ma14112942.
[18] A.P.S. Brogan, L. Bui-Le, J.P. Hallett, Non-aqueous homogenous biocatalytic conversion of polysaccharides in ionic liquids using chemically modified glucosidase, Nat. Chem. 10 (2018) 859–865, https://doi.org/10.1038/s41557-018-0088-6.
[19] M.K. Tran, M.T.F. Rodrigues, K. Kato, G. Babu, P.M. Ajayan, Deep eutectic solvents for cathode recycling of Li-ion batteries, Nat. Energy 4 (2019) 339–345, https://doi.org/10.1038/s41560-019-0368-4.
[20] S. Azmi, M.F. Koudahi, E. Frackowiak, Reline deep eutectic solvent as a green electrolyte for electrochemical energy storage applications†, Energy Environ. Sci. 15 (2022) 1156–1171, https://doi.org/10.1039/d1ee02920g.
[21] N. López-Salas, D. Carriazo, M.C. Gutiérrez, M.L. Ferrer, C.O. Ania, F. Rubio, A. Tamayo, J.L.G. Fierro, F. Del Monte, Tailoring the textural properties of hierarchical porous carbons using deep eutectic solvents, J. Mater. Chem. A. 4 (2016) 9146–9159, https://doi.org/10.1039/c6ta02704k.
[22] C.L. Boldrini, A.F. Quivelli, N. Manfredi, V. Capriati, A. Abbotto, Deep eutectic solvents in solar energy technologies, Molecules 27 (2022) 1–20, https://doi.org/10.3390/molecules27030709.
[23] X. Ge, C. Gu, X. Wang, J. Tu, Deep eutectic solvents (DESs)-derived advanced functional materials for energy and environmental applications: challenges, opportunities, and future vision, J. Mater. Chem. A. 5 (2017) 8209–8229, https://doi.org/10.1039/c7ta01659j.
[24] S.N. Rashid, A. Hayyan, M. Hayyan, M.A. Hashim, A.A.M. Elgharbawy, F.S. Sani, W.J. Basirun, V.S. Lee, Y. Alias, A.K. Mohammed, M.E.S. Mirghani, M. Y. Zulkifli, M. Rageh, Ternary glycerol-based deep eutectic solvents: physicochemical properties and enzymatic activity, Chem. Eng. Res. Des. 169 (2021) 77–85, https://doi.org/10.1016/j.cherd.2021.02.032.
[25] H. Kivelä, M. Salomäki, P. Vainikka, E. Mäkilä, F. Poletti, S. Ruggeri, F. Terzi, J. Lukkari, Effect of water on a hydrophobic deep eutectic solvent, J. Phys. Chem. B 126 (2022) 513–527, https://doi.org/10.1021/acs.jpcb.1c08170.
[26] Y. Wang, H. Zhou, A green and cost-effective rechargeable battery with high energy density based on a deep eutectic catholyte, Energy Environ. Sci. 9 (2016) 2267–2272, https://doi.org/10.1039/c6ee00902f.
[27] R. Saputra, R. Walvekar, M. Khalid, N.M. Mubarak, Synthesis and thermophysical properties of ethylammonium chloride-glycerol-ZnCl2 ternary deep eutectic solvent, J. Mol. Liq. 310 (2020), 113232, https://doi.org/10.1016/j.molliq.2020.113232.
[28] M. Zhang, X. Zhang, Y. Liu, K. Wu, Y. Zhu, H. Lu, B. Liang, Insights into the relationships between physicochemical properties, solvent performance, and applications of deep eutectic solvents, Environ. Sci. Pollut. Res. 28 (2021) 35537–35563, https://doi.org/10.1007/s11356-021-14485-2.
[29] Z. Chen, M. Ludwig, G.G. Warr, R. Atkin, Effect of cation alkyl chain length on surface forces and physical properties in deep eutectic solvents, J. Colloid Interface Sci. 494 (2017) 373–379, https://doi.org/10.1016/j.jcis.2017.01.109.
[30] M.H. Shafie, R. Yusof, C.Y. Gan, Synthesis of citric acid monohydrate-choline chloride based deep eutectic solvents (DES) and characterization of their physicochemical properties, J. Mol. Liq. 288 (2019), 111081, https://doi.org/10.1016/j.molliq.2019.111081.
[31] K. Sarjuna, D. Ilangeswaran, Preparation of some zinc chloride based deep eutectic solvents and their characterization, Mater. Today Proc. 33 (2020) 2767–2770, https://doi.org/10.1016/j.matpr.2020.02.080.
[32] M. Khalid, M. Hayyan, M. Abdulhakim, S. Akib, Glycerol-based deep eutectic solvents : physical properties, J. Mol. Liq. 215 (2016) 98–103, https://doi.org/10.1016/j.molliq.2015.11.032.
[33] A. Cushing, T. Zheng, K. Higa, G. Liu, Viscosity analysis of battery electrode slurry, Polymers 13 (2021) 1–8, https://doi.org/10.3390/polym13224033.
[34] A.K. Jangir, P. Sethy, G. Verma, P. Bahadur, K. Kuperkar, An inclusive thermophysical and rheology portrayal of deep eutectic solvents (DES) for metal oxides dissolution enhancement, J. Mol. Liq. 332 (2021), 115909, https://doi.org/10.1016/j.molliq.2021.115909.
[35] A. Basaiahgari, S. Panda, R.L. Gardas, Effect of ethylene, diethylene, and triethylene glycols and glycerol on the physicochemical properties and phase behavior of benzyltrimethyl and benzyltributylammonium chloride based deep eutectic solvents at 283.15-343.15 K, J. Chem. Eng. Data 63 (2018) 2613–2627, https://doi.org/10.1021/acs.jced.8b00213.
[36] N. Delgado-Mellado, M. Larriba, P. Navarro, V. Rigual, M. Ayuso, J. García, F. Rodríguez, Thermal stability of choline chloride deep eutectic solvents by TGA/FTIR-ATR analysis, J. Mol. Liq. 260 (2018) 37–43, https://doi.org/10.1016/j.molliq.2018.03.076.
[37] Y. Wang, Z. Niu, Q. Zheng, C. Zhang, J. Ye, G. Dai, Y. Zhao, X. Zhang, Zn-based eutectic mixture as anolyte for hybrid redox flow batteries, Sci. Rep. 8 (2018) 8–15, https://doi.org/10.1038/s41598-018-24059-x.
[38] W. Wu, Q. Li, M. Cao, D. Li, J. Lu, M. Li, J. Zhang, Non-flammable dual-salt deep eutectic electrolyte for high-voltage lithium metal battery, Crystals 12 (2022) 1–9, https://doi.org/10.3390/cryst12091290.
[39] L. Zhang, G. Yu, L. Zhang, C. Zhang, Y. Ding, K. Ramirez-meyers, G. Yu, A low-cost and high-energy hybrid iron- aluminum liquid battery achieved by deep eutectic solvents a low-cost and high-energy hybrid iron-aluminum liquid battery achieved by deep eutectic solvents, Joule. 1 (n.d.) 623–633. https://doi.org/10.1016/j.joule.2017.08.013.
[40] M.A. Kadhom, G.H. Abdullah, N. Al-Bayati, Studying two series of ternary deep eutectic solvents (choline chloride–urea–glycerol) and (choline chloride–malic acid–glycerol), synthesis and characterizations, Arabian J. Sci. Eng. 42 (2017) 1579–1589, https://doi.org/10.1007/s13369-017-2431-4.
[41] M. Salari, J.C. Varela, H. Zhang, M.W. Grinstaff, Sustainable glycerol carbonate electrolytes for Li-ion supercapacitors: performance evaluation of butyl, benzyl, and ethyl glycerol carbonates, Mater. Adv. 2 (2021) 6049–6057, https://doi.org/10.1039/d1ma00547b.
[42] Q. Xu, T.S. Zhao, L. Wei, C. Zhang, X.L. Zhou, Electrochemical characteristics and transport properties of Fe(II)/Fe(III) redox couple in a non-aqueous reline deep eutectic solvent, Electrochim. Acta 154 (2015) 462–467, https://doi.org/10.1016/j.electacta.2014.12.061.
[43] R. Cheng, J. Xu, X. Wang, Q. Ma, H. Su, W. Yang, Q. Xu, Electrochemical characteristics and transport properties of V(II)/V(III) redox couple in a deep eutectic solvent: magnetic field effect, Front. Chem. 8 (2020) 1–11, https://doi.org/10.3389/fchem.2020.00619.
[44] S. Azizighannad, Z. Wang, Z. Siddiqui, V. Kumar, S. Mitra, Nano carbon doped polyacrylamide gel electrolytes for high performance supercapacitors, Molecules 26 (2021), https://doi.org/10.3390/molecules26092631.